Proton mass decomposition

Yi-Bo Yang[1,⋆], *Ying* Chen[2], *Terrence* Draper[3], *Jian* Liang[3], and *Keh-Fei* Liu[3]

[1] *Department of Physics and Astronomy, Michigan State University, East Lansing, MI 48824, USA*
[2] *Institute of High Energy Physics and Theoretical Physics Center for Science Facilities, Chinese Academy of Sciences, Beijing 100049, China*
[3] *Department of Physics and Astronomy, University of Kentucky, Lexington, KY 40506, USA*

Abstract. We report the results on the proton mass decomposition and also on the related quark and glue momentum fractions. The results are based on overlap valence fermions on four ensembles of $N_f = 2 + 1$ DWF configurations with three lattice spacings and volumes, and several pion masses including the physical pion mass. With 1-loop perturbative calculation and proper normalization of the glue operator, we find that the u, d, and s quark masses contribute 9(2)% to the proton mass. The quark energy and glue field energy contribute 31(5)% and 37(5)% respectively in the $\overline{MS}$ scheme at $\mu = 2$ GeV. The trace anomaly gives the remaining 23(1)% contribution. The u, d, s and glue momentum fractions in the $\overline{MS}$ scheme are consistent with the global analysis at $\mu = 2$ GeV.

1 Introduction

The Higgs boson provides the source of quark masses. But how it is related to the proton mass and thus the mass of nuclei and atoms is another question. The masses of the valence quarks in the proton are just ∼3 MeV per quark which is directly related to the Higgs boson, while the total proton mass is 938 MeV. How large the quark and gluon contributions to the proton mass are, is a question that can only answered by solving QCD nonperturbatively, and/or with information from experiment. With phenomenological input, the first decomposition was carried out by Ji over twenty years ago [1]. As in Ref. [1, 2], the Hamiltonian of QCD can be decomposed as

$$M = -\langle T_{44}\rangle = \langle H_m\rangle + \langle H_E\rangle(\mu) + \langle H_g\rangle(\mu) + \langle H_a\rangle, \tag{1}$$

and the trace anomaly gives

$$M = -4\,\langle \hat{T}_{44}\rangle = \langle H_m\rangle + 4\,\langle H_a\rangle, \tag{2}$$

with H_m, H_E, and H_g denoting the contributions from the quark mass, the quark energy, and the glue field energy, respectively:

$$\begin{aligned} H_m &= \sum_{u,d,s\cdots}\int d^3x\, m\,\overline{\psi}\psi, \quad H_E = \sum_{u,d,s\ldots}\int d^3x\,\overline{\psi}(\vec{D}\cdot\vec{\gamma})\psi, \\ H_g &= \int d^3x\,\frac{1}{2}(B^2 - E^2), \end{aligned} \tag{3}$$

⋆Speaker, e-mail: yangyibo@pa.msu.edu

and the QCD anomaly term H_a is the joint contribution from the quantum anomaly of both glue and quark,

$$H_a = H_g^a + H_m^\gamma, \quad H_g^a = \int d^3x \, \frac{-\beta(g)}{4g}(E^2 + B^2), \quad H_m^\gamma = \sum_{u,d,s\cdots} \int d^3x \, \frac{1}{4}\gamma_m m \overline{\psi}\psi. \tag{4}$$

All the $\langle H \rangle$ are defined by $\langle N|H|N\rangle/\langle N|N\rangle$ where $|N\rangle$ is the nucleon state in the rest frame. Note that $\langle H_E + H_g\rangle$, $\langle H_m\rangle$ and $\langle H_a\rangle$ are scale and renormalization scheme independent, but $\langle H_E\rangle(\mu)$ and $\langle H_g\rangle(\mu)$ separately have scale dependence.

The nucleon mass M can be calculated from the nucleon two-point function. If one calculates further $\langle H_m\rangle$ and $\langle H_E\rangle(\mu)$, then $\langle H_g\rangle(\mu)$ and $\langle H_a\rangle$ can be obtained through Eqs. (1) and (2). The approach has been adopted to decompose the S-wave meson masses to gain insight about contributions of each term from light mesons to charmonuims [2]. In this work, the quark energy $\langle H_E\rangle$ is obtained from the quark momentum fraction from a local current and $\langle H_m\rangle$ and with the help of the equation of motion, i.e.

$$\langle H_E\rangle = \frac{3}{4}\langle x\rangle_q M - \frac{3}{4}\langle H_m\rangle. \tag{5}$$

Since there is an $O(a^2)$ error in the equation of motion due to the fact that the local energy-momentum tensor operator adopted is not the conserved current, the concomitant systematic error can be up to 20% for the light quark case in the meson mass study of the pseudoscalar meson [2]. In principle, it would be better to use the conserved energy-momentum tensor (EMT) on the lattice to avoid the need for normalization and attempts to construct such a conserved EMT on the lattice have been made perturbatively and non-perturbatively [3] and recently by Suzuki [4, 5] with gradient flow at finite lattice spacing. However, they are complicated to construct. In the present work, we still use the local current and will address the normalization in addition to renormalization and mixing.

In addition to calculating the quark momentum fraction $\langle x\rangle_q$, we also calculate the glue momentum fraction $\langle x\rangle_g$. The latter is directly related to the glue field energy

$$\langle H_g\rangle = \frac{3}{4}\langle x\rangle_g M. \tag{6}$$

We will discuss the normalization, renormalization, and mixing of $\langle x\rangle_q$ and $\langle x\rangle_g$ later.

In this proceeding, we will calculate the renormalized quark and glue momentum fractions in the proton on four lattice ensembles and interpolate the results to the physical pion mass with a global fit including finite lattice spacing and volume corrections. Then we will combine the previous $\langle H_m\rangle$ result [6] to obtain the full decomposition of the proton mass.

2 Numerical setup

We use overlap valence fermion on $(2+1)$ flavor RBC/UKQCD DWF gauge configurations from four ensembles on $24^3 \times 64$ (24I), $32^3 \times 64$ (32I) [7], $32^3 \times 64$ (32ID) and $48^3 \times 96$ (48I) [8] lattices. These ensembles cover three values of the lattice spacing and volume, and four values of the quark mass in the sea, and then allow us to implement a global fit on our results to control the systematic uncertainties as in Ref. [6, 9]. Other parameters of the ensembles used are listed in Table 1.

The effective quark propagator of the massive overlap fermion is the inverse of the operator $(D_c + m)$ [10, 11], where D_c is chiral, i.e. $\{D_c, \gamma_5\} = 0$ [12] and its detailed definition can be found in our previous works [13–15]. We used 5 quark masses from the range $m_\pi \in (250, 400)$ MeV on the 24I and 32I ensembles, and 6 quark masses from $m_\pi \in (140, 400)$ MeV on the other two ensembles which have larger volumes and thus allow a lighter pion mass with the constraint $m_\pi L > 3.8$. For all the

Table 1. The parameters for the RBC/UKQCD configurations[8]: spatial/temporal size, lattice spacing, the sea strange quark mass under $\overline{MS}$ scheme at 2 GeV, the pion mass with the degenerate light sea quark (both in unit of MeV), and the number of configurations used in this proceeding.

Symbol	$L^3 \times T$	a (fm)	$m_s^{(s)}$	m_π	N_{cfg}
24I	$24^3 \times 64$	0.1105(3)	120	330	203
32I	$32^3 \times 64$	0.0828(3)	110	300	309
32ID	$32^3 \times 64$	0.1431(7)	89.4	171	200
48I	$48^3 \times 96$	0.1141(2)	94.9	139	81

quark propagators, 1 step of HYP smearing is applied on all the configurations to improve the signal. Numerical details regarding the calculation of the overlap operator, eigenmode deflation in inversion of the quark matrix, and the $Z(3)$ grid smeared source with low-mode substitution (LMS) to increase statistics are given in [13–15].

The matrix elements we need are obtained from the ratio of the three-point function to the two-point function

$$R(t_f, t) = \frac{\langle 0| \int d^3y \Gamma^e \chi(\vec{y}, t_f) \mathcal{O}(t) \sum_{\vec{x}\in G} \bar{\chi}_S(\vec{x}, 0)|0\rangle}{\langle 0| \int d^3y \Gamma^e \chi(\vec{y}, t_f) \sum_{\vec{x}\in G} \bar{\chi}_S(\vec{x}, 0)|0\rangle}, \tag{7}$$

where χ is the standard proton interpolation field and $\bar{\chi}_S$ is the field with gaussian smearing applied to all three quarks. All the correlation functions from the source points $\vec{x}$ in the grid G are combined to improve the the signal-to-noise ratio (SNR). $\mathcal{O}(t)$ is the current operator located at time slice t and Γ^e is the unpolarized projection operator of the nucleon. When t_f is large enough, $R(t_f, t)$ approaches the bare nucleon matrix element matrix element $\langle N|\mathcal{O}|N\rangle$.

For each quark mass on each ensemble, we construct $R(t_f, t)$ for several sink-source separations t_f from 0.7 fm to 1.5 fm and all the current insertion times t between the source and sink, combine all the data to do the two-state fit, and then obtain the matrix elements we want with the excited-states contamination under control. The more detailed discussion of the simulation setup and the two-state fit can be found in our previous work [6, 9, 16].

To improve the signal in the disconnected insertion case needed for the gluon, strange and also the light sea quarks cases, all the time slices are looped over for the proton two-point functions. With 5 steps of the HYP smearing, the signal of the glue operator is further improved as evidenced in Ref. [16].

3 Results

The quark and gluon momentum fractions in the nucleon can be defined by the traceless diagonal part of the EMT matrix element in the rest frame [17],

$$\begin{aligned} \langle x \rangle_{q,g}^{\rm tr} &\equiv \frac{\mathrm{Tr}[\Gamma^e \langle N| \frac{4}{3} \bar{T}_{44}^{q,g} |N\rangle]}{M \mathrm{Tr}[\Gamma^e \langle N|N\rangle]}, \\ \bar{T}_{44}^q &= \int d^3x \bar{\psi}(x) \frac{1}{2} (\frac{3}{4} \gamma_4 \overleftrightarrow{D}_4 - \frac{1}{4} \sum_{i=1,2,3} \gamma_i \overleftrightarrow{D}_i) \psi(x), \quad \bar{T}_{44}^g = \int d^3x \frac{1}{2} (B(x)^2 - E(x)^2), \end{aligned} \tag{8}$$

where M is the proton mass, or alternatively by the off-diagonal part of the EMT matrix elements,

$$\langle x\rangle^{\rm off}_{q,g} \equiv \frac{{\rm Tr}[\Gamma^e\langle P|T^{q,g}_{4i}|P\rangle]}{P_i{\rm Tr}[\Gamma^e\langle P|P\rangle]} \qquad (9)$$
$$T^q_{4i} = \int d^3x\bar{\psi}(x)\frac{1}{4}\gamma_{\{4}\overleftrightarrow{D}_{i\}}\psi(x),\quad T^g_{4i} = \int d^3x\epsilon_{ijk}E_j(x)B_k(x),$$

where $|P\rangle$ is the nucleon state with momentum P and P_i is a non-zero component of P. These two definitions should give the same result in the continuum due to the rotational symmetry. But they can be different under the lattice regularization which breaks this symmetry and should be renormalized separately to get consistent results.

In Ref. [18], we provided the 1-loop renormalization and mixing calculation of $\bar{T}_{44}$ and $\bar{T}_{4i}$. The rotational symmetry breaking effects in the renormalization constant of the quark operator and the mixing from quark to gluon are small, while that in the gluon to quark mixing case is large. The glue renormalization constant turns out to be ∼2 at the 1-loop level and is thus not reliable. The renormalization condition provided in Ref. [18] can also be used for the non-perturbative renormalization calculation, and the preliminary result shows that the renormalization constant of the gluon operator with 1-step HYP smearing is about 1.3 [19]. That with more steps of the HYP smearing is under investigation and would be closer to 1, since the corresponding bare gluon matrix elements are slightly increased compared to the 1-step HYP smearing case.

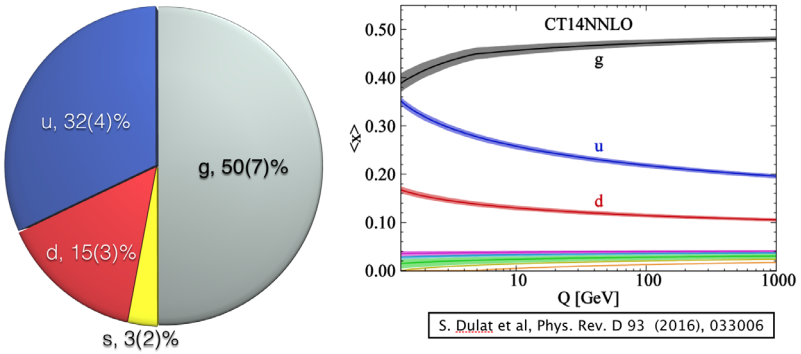

Figure 1. The contributions of different quark flavors and glue to the proton momentum fraction. The left panel shows the lattice results renormalized in the $\overline{\rm MS}$ scheme at 2 GeV with 1-loop perturbative calculation and proper normalization of the glue. The experimental values are illustrated in the right panel, as a function of the $\overline{\rm MS}$ scale. Our results agree with the experimental values at 2 GeV.

In view of the uncertainty in the glue renormalization, we calculate the renormalized quark momentum fractions with the 1-loop perturbative calculation including the mixing of the bare glue momentum fraction and apply the momentum sum rule to determine the renormalized glue momentum fraction. The resulting renormalized momentum fractions of the u, d, s quarks, and glue in the $\overline{\rm MS}$ scheme at 2 GeV are illustrated in the left panel of Fig. 1, while the right panel shows the corresponding experimental values as a function of Q [20]. We note that they agree with each other well within uncertainties.

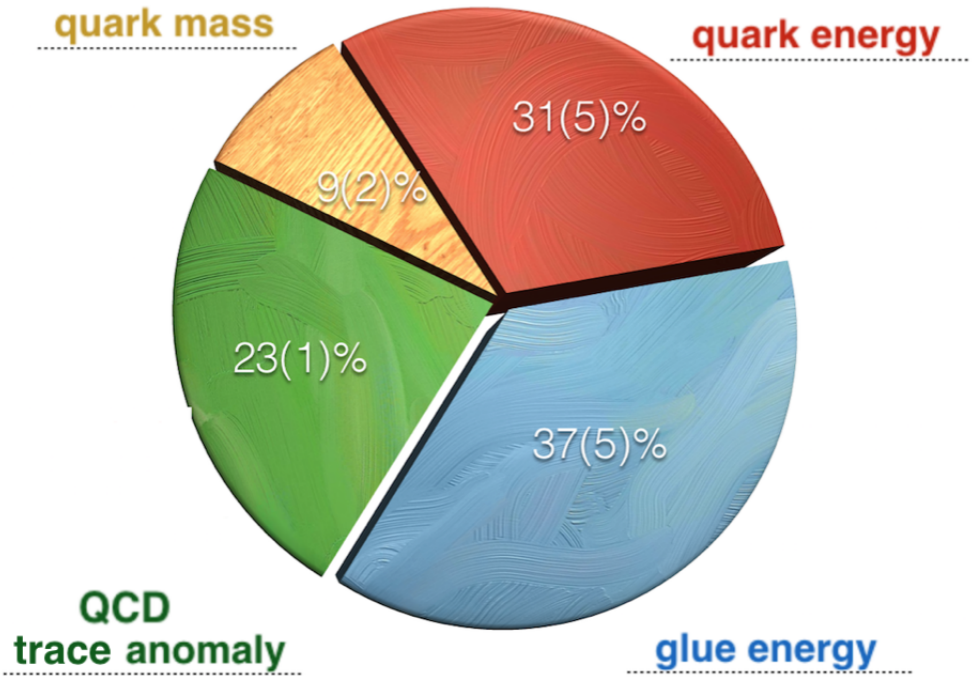

Figure 2. The pie chart of the proton mass decomposition, in terms of the quark mass, quark energy, glue field energy and trace anomaly.

With these momentum fractions, we can apply Eqs. (5) and (6) to obtain the quark and glue energy contributions in the proton mass, and combine with the quark mass contribution [6] to obtain the entire picture of the proton mass decomposition, as illustrated in Fig. 2.

4 Summary

In summary, we present a simulation strategy to calculate the proton mass decomposition. The renormalization and mixing between the quark and glue energy can be calculated perturbatively or non-perturbatively, while the quark mass contribution and the trace anomaly are renormalization group invariant. Based on this strategy, the lattice simulation is processed on four ensembles with three lattice spacings and volumes, and several pion masses including the physical pion mass, to control the systematic uncertainties. With 1-loop perturbative calculation and proper normalization on the glue, we obtained the proton mass decomposition, with the quark mass and trace anomaly contributing 9(2)% and 23(1)% respectively, while the fractional contributions of the quark and glue field energies are 31(5)% and 37(5)% in the $\overline{\text{MS}}$ scheme at 2 GeV. As a check of validity of the present calculation,

we find that the individual u, d, s and glue momentum fractions compare favorably with those from the global fit in the $\overline{\text{MS}}$ scheme at 2 GeV.

References

[1] X.D. Ji, Phys. Rev. Lett. **74**, 1071 (1995), hep-ph/9410274
[2] Y.B. Yang, Y. Chen, T. Draper, M. Gong, K.F. Liu, Z. Liu, J.P. Ma, Phys. Rev. **D91**, 074516 (2015), 1405.4440
[3] S. Caracciolo, G. Curci, P. Menotti, A. Pelissetto, Annals Phys. **197**, 119 (1990)
[4] H. Suzuki, PTEP **2013**, 083B03 (2013), [Erratum: PTEP2015,079201(2015)], 1304.0533
[5] H. Makino, H. Suzuki, PTEP **2014**, 063B02 (2014), [Erratum: PTEP2015,079202(2015)], 1403.4772
[6] Y.B. Yang, A. Alexandru, T. Draper, J. Liang, K.F. Liu (xQCD), Phys. Rev. **D94**, 054503 (2016), 1511.09089
[7] Y. Aoki et al. (RBC, UKQCD), Phys. Rev. **D83**, 074508 (2011), 1011.0892
[8] T. Blum et al. (RBC, UKQCD), Phys. Rev. **D93**, 074505 (2016), 1411.7017
[9] R.S. Sufian, Y.B. Yang, A. Alexandru, T. Draper, J. Liang, K.F. Liu, Phys. Rev. Lett. **118**, 042001 (2017), 1606.07075
[10] T.W. Chiu, Phys. Rev. **D60**, 034503 (1999), hep-lat/9810052
[11] K.F. Liu, Int. J. Mod. Phys. **A20**, 7241 (2005), hep-lat/0206002
[12] T.W. Chiu, S.V. Zenkin, Phys. Rev. **D59**, 074501 (1999), hep-lat/9806019
[13] A. Li et al. (χQCD), Phys. Rev. **D82**, 114501 (2010), 1005.5424
[14] M. Gong et al. (χQCD), Phys. Rev. **D88**, 014503 (2013), 1304.1194
[15] Y.B. Yang, A. Alexandru, T. Draper, M. Gong, K.F. Liu, Phys. Rev. **D93**, 034503 (2016), 1509.04616
[16] Y.B. Yang, R.S. Sufian, A. Alexandru, T. Draper, M.J. Glatzmaier, K.F. Liu, Y. Zhao, Phys. Rev. Lett. **118**, 102001 (2017), 1609.05937
[17] R. Horsley, R. Millo, Y. Nakamura, H. Perlt, D. Pleiter, P.E.L. Rakow, G. Schierholz, A. Schiller, F. Winter, J.M. Zanotti (UKQCD, QCDSF), Phys. Lett. **B714**, 312 (2012), 1205.6410
[18] Y.B. Yang, M. Glatzmaier, K.F. Liu, Y. Zhao (2016), 1612.02855
[19] Y.B. Yang, In preparation (2017)
[20] S. Dulat, T.J. Hou, J. Gao, M. Guzzi, J. Huston, P. Nadolsky, J. Pumplin, C. Schmidt, D. Stump, C.P. Yuan, Phys. Rev. **D93**, 033006 (2016), 1506.07443